Proceedings of the ASME 2010 3rd Joint US-European Fluids Engineering Summer Meeting and 8th International Conference on Nanochannels, Microchannels, and Minichannels
FEDSM-ICNMM2010
August 1-5, 2010, Montreal, Canada

FEDSM-ICNMM2010-30505

FLOW OF A THIN VISCOELASTIC JET

Moinuddin Ahmed[1] and Roger E.Khayat[1]
[1]Department of Mechanical and Materials Engineering, The University of Western Ontario
London, Ontario N6H 1R7, Canada.

Email: mahmed84@uwo.ca

ABSTRACT

The influence of elasticity and inertia for steady flow of a thin viscoelastic fluid jet is examined theoretically. The fluid is assumed to emerge from a vertical channel and driven by a pressure gradient and/or gravity. The boundary-layer equations are generalized for a viscoelastic thin film obeying the Oldroyd-b constitutive model**.** Special emphasis is placed on the initial stages of jet development. The formulation and simulation are carried out for two-dimensional jet flow in order to better understand the intricate wave and flow structures for a viscoelastic jet. In contrast to the commonly used depth-averaging solution method, the strong nonlinearities are preserved in the present formulation as the viscoelastic boundary-layer equations are solved by expanding the flow field in terms of orthonormal shape functions. It is found that for a steady viscoelastic jet, a reduction in inertia or a rise in elasticity leads to the emergence of surface waviness and excessive normal stress, which leads to the formation of sharp gradients in the velocity and shear stress. These gradients can be sufficiently substantial to cause a discontinuity or shock in the flow. During transition, the surface profiles adhere earlier to the shape of the final steady state instead of a traveling wave, the transition between the two states takes the form of a standing wave, which grows essentially in amplitude only.

INTRODUCTION

This study examines the role of elasticity and inertia for steady flow of a viscoelastic fluid jet emerging from a vertical channel. The study of liquid laminar jets has been extensively examined previously in the literature. However, the focus has mainly been on steady Newtonian jet flow. This is primarily because it is the long-term behavior of the flow, after transient effects have subsided that is generally important. In contrast, when instances of irregularity and instability occur, it is usually the initial stages of development, long before the process reaches steady state, which can be traced to the origin of the instability. The time taken for a fluid to reach steady state is also of importance. Because polymeric fluids exhibit different relaxation times, they will therefore display different transient responses. There are many studies devoted to the modeling and simulation of jet flows. Appreciatively, jet flow has been predominantly examined for Newtonian fluids (Chang[8] 1994), and to a much lesser extent for non-Newtonian film flow (for instance Bérdaudo[3] et al. 1998, and the references therein). The present theoretical study is focused on the planar flow of a thin viscoelastic jet emerging from a channel. Special emphasis is placed on the initial stages of jet development, with the overall influence of inertia, elasticity and gravity examined for both steady and transient jet flow.

Generally, for small inertia flow of a Newtonian film, Benney's[2] (1966) long wave (LW) approximation is often used. At first glance, the LW approximation appears to be a suitable choice for the modeling of viscoelastic jet flow. However, the LW approximation becomes seriously limited in the presence of moderate or high inertia (Chang[8] 1994). One may then safely speculate that a similar limitation will be encountered for moderate or highly elastic film flow. For a Newtonian film, the LW approximation at Re >> 1 is typically not valid, and it is generally found that in this case, inertial effects are better represented using the boundary-layer (BL) formulation. Typically, an ad-hoc simplification of the BL solution is achieved using a self-similar parabolic flow profile (Shkadov[22] 1967, 1968). This amounts to depth-averaging the BL equations, which in the limit of creeping flow, leads to an exact formulation. Although this process circumvents the difficulty inherent to the LW approximation (Demekhin & Shkadov[10] 1985, Trifonov & Tsvelodu[26] 1991, Chang[7] et al 1993), the self-similar behavior is not expected to hold in the presence of high inertia or normal stress effects. The solution of the BL equations remains essentially as difficult as that of the

Navier-Stokes equations. The depth-averaging method leads to a second-order accurate solution in time, yielding plausible results, but raises a certain level of doubt in the presence of strong convective (and upper-convective) nonlinearities due to the semi-parabolic assumption (Frenkel[12] 1992). The parabolic approximation is widely used in the literature and its validity was established experimentally by Alekseenko, Narkoryakov, & Pokusaev[1] (1985). However, it is generally argued that this validity holds only at low Reynolds number and provided that the surface waves are far from the entry (Wilkes[28] 1962; Bertshy & Chin[4] 1993). High inertia flow, turbulence, the presence of end effects, nonlinear effects stemming from shear-thinning or viscoelastic effects are all factors that challenge the validity of the semi-parabolic profile.

The free-surface flow of non-Newtonian fluids remains generally challenging. This is also true for thin film flow. Bérdaudo[3] et al (1998) examined the free-surface flow of a viscoelastic fluid emerging from various geometries. Kang & Chen[13] (1995) studied gravity-driven non-Newtonian films as well as creeping flow in the presence of surface tension effect. The planar flow of a Newtonian film was first considered over a stationary substrate (Khayat & Welke[15] 2001; Khayat & Kim[16] 2002) and a moving substrate (Tauqueer & Khayat[23] 2004). The coating of shear-thinning (Kim and Khayat[18] 2002) and viscoelastic (Khayat[14] 2001) fluids were also considered on a planar substrate, and on axisymmetric substrates (Khayat & Kim[17] 2006). Regarding the jet flow of viscoelastic fluids, the focus has mainly been in the literature on die swell and steady flow (for instance, Trang-Cong & Phan-Thien[25] 1988, and, more recently, Liang[20] 1995). Tome, Duffy & McKee[24] (1996) examined the transient die swell and buckling of planar jets for Newtonian and generalized Newtonian fluids. Surface tension jet breakup of non-Newtonian fluids have also been examined both experimentally (Christanti & Walker[9] 2001) and theoretically (Bousfield, Keunings, Marrucci & Denn[6] 1986). The transient response resulting from the spreading of surfactant on a thin weakly viscoelastic film has also been examined theoretically by Zhang, Matar & Craster[29] (2002).

In the present study, the formulation and simulation are carried out for two-dimensional jet flow in order to better understand the intricate wave and flow structures for a viscoelastic jet. The problems associated with frequent mesh resizing needed for the rapid spatio-temporal variations in the flow field make conventional solutions schemes such as finite-element/difference methods unsuitable. For the pressure/gravity driven flow in this study, a spectral approach is adopted for a viscoelastic fluid with a generalized BL formulation proposed. The system is first mapped onto a rectangular domain, followed by the expansion of the velocity field in terms of orthonormal basis functions. The Galerkin projection is used to derive the equations that govern the coefficients of expansion, which are then integrated numerically. This formulation is similar to the one adopted by Khayat & Kim[17] (2006) for coating flow, and by German & Khayat[11] (2005) for thin-jet flow of a Newtonian fluid. Unlike the depth-averaging method, the spectral methodology proposed becomes particularly suited for the early onset of wave propagation near the channel exit in the presence of strong normal-stress effect.

NOMENCLATURE

a = Solute-to-solution ratio
Ca = Capillary number
De = Deborah number
Fr = Froude number
G = Gravity number
g = Gravitational acceleration
P = Hydrostatic pressure
q = Streamwise normal stress
r = Transverse normal stress
Re = Reynolds number
Rv = Solvent-to-solute ratio
s = Shear stress
T = Time
U = Velocity vector
∇ = Gradient operator
ε = Aspect ratio
λ = Relaxation time
μ = Fluid viscosity
μ_s = Newtonian solvent viscosity
μ_p = Polymeric solute viscosity
ρ = Fluid density
$\mathbf{\Sigma}$ = Stress tensor

GOVERNING EQUATIONS, BOUNDARY AND INITIAL CONDITIONS

In this section, the governing equations are introduced, including the scaled conservation and constitutive equations, as well as the boundary and initial conditions for a viscoelastic thin fluid jet.

The fluid examined in this study is assumed to be an incompressible polymeric solution represented by a single relaxation time and constant viscosity. The fluid properties include the density, viscosity and relaxation time. Regardless of the nature of the fluid, the continuity and momentum conservation equations must hold. For an incompressible fluid, the conservation equations are:

$$\nabla \cdot \boldsymbol{U} = 0, \quad \rho\left(\boldsymbol{U}_{\mathrm{T}} + \boldsymbol{U} \cdot \nabla \boldsymbol{U}\right) = \nabla \cdot \boldsymbol{\Sigma} + \rho \boldsymbol{g} \tag{1}$$

There are two components making up the deviatoric part of the stress tensor, a Newtonian constituent (solvent), and a polymeric constituent (solute). The stress tensor is then expressed as;

$$\Sigma = -\mathrm{P}\boldsymbol{I} + \mu_{\mathrm{s}}\left(\nabla \boldsymbol{U} + \nabla \boldsymbol{U}^{\mathrm{T}}\right) + \boldsymbol{T} \tag{2}$$

Where matrix transposition is denoted by superscript T.

The polymeric constitutive equation for $\boldsymbol{T}$ is taken to correspond to an Oldroyd-B fluid and is written in the form (Bird, Armstrong & Hassanger[5] 1987):

$$\lambda\left(\boldsymbol{T}_{\mathrm{T}}+\boldsymbol{U}\cdot\nabla\boldsymbol{T}-\boldsymbol{T}\cdot\nabla\boldsymbol{U}-\nabla\boldsymbol{U}^{\mathrm{T}}\cdot\boldsymbol{T}\right)+\boldsymbol{T}=\mu_{\mathrm{p}}\left(\nabla\boldsymbol{U}+\nabla\boldsymbol{U}^{\mathrm{T}}\right) \quad (3)$$

The equation for a Maxwell fluid is recovered in the limit $\mu_s \rightarrow 0$ in equations (1) to (3), and the limit $\mu_p \rightarrow 0$ leads to the Navier-Stokes equations. The problem is now examined using a Cartesian coordinate system using standard notations for velocity and stress components.

The flow of a viscoelastic jet emerging from a channel is schematically depicted in fig. 1 in the (X, Z) plane.

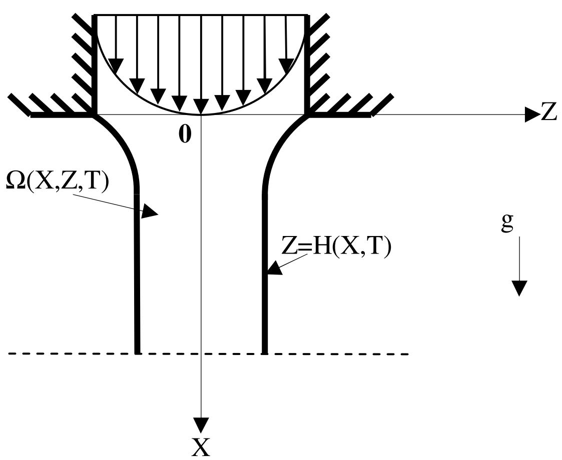

FIGURE 1: SCHEMATIC ILLUSTRATION OF TWO-DIMENSIONAL JET FLOW EMERGING FROM A VERTICAL CHANNEL.

The X-axis is chosen to correspond to the vertical (streamwise) direction and the Z-axis is chosen in the horizontal (transverse) direction. The domain of the fluid is represented by Ω(X, Z, T), with the (half) jet thickness denoted by Z = H(X, T). The channel exit coincides with X = 0, and the (symmetric) flow is examined in the (X, Z) plane, with Z = 0 corresponding to the line of symmetry. The flow is induced by either a pressure gradient inside the channel and/or gravity, but for this study the emphasis will be on pressure-driven flow. The streamwise and transverse scale lengths are chosen to be a suitably defined length L, and the channel half width H_0, respectively. Since the film half thickness is of the same order as the boundary layer thickness, then $L\sim\dfrac{\rho U_0 H_0^{\,2}}{\mu}$. For both Newtonian and non-Newtonian fluids, there are four main dimensionless parameters. Explicitly written, these take the following form:

$$Re=\frac{\rho U_0 H_0^{\,2}}{\mu L}, \quad \varepsilon=\frac{H_0}{L}, \quad Fr=\frac{U_0}{\sqrt{gL}}, \quad Ca=\frac{\mu U_o}{\sigma}$$

where the reference velocity, U_0, is the mean velocity in the channel in the absence of gravity. Note, in this case, that $Re\sim O(1)$ and $\varepsilon\sim O\left(Re_H^{-1}\right)$, where Re_H is the Reynolds based on H_0. Additional to these parameters are the similarity parameters for a viscoelastic flow, which include:

$$De=\frac{\lambda U_0}{L}, \quad Rv=\frac{\mu_s}{\mu_p}, \quad a=\frac{\mu_p}{\mu}=\frac{1}{Rv+1}$$

In this study, the fluid film is assumed thin with $\varepsilon << 1$. Thus, ε is taken as the perturbation parameter in order to reduce the formulation to that of the boundary-layer type. The scaling of the velocity, shear and normal stresses, and position coordinates take the following non-dimensional form:

$$x=\frac{X}{L}, \quad z=\frac{Z}{H_0}, \quad t=\frac{U_0 T}{L}, \quad p=\frac{PL\varepsilon^2}{\mu U_0}$$
$$u=\frac{U}{U_0}, \quad w=\frac{W}{\varepsilon U_0}, \quad h=\frac{H}{H_0}$$

The nonlinearities in the upper-convective terms create difficulty when scaling the stress equations. In general, one may set:

$$q=\frac{L\varepsilon^{\alpha}}{\mu U_0}T_{xx}, \quad s=\frac{L\varepsilon^{\beta}}{\mu U_0}T_{xz}, \quad r=\frac{L\varepsilon^{\gamma}}{\mu U_0}T_{zz}$$

Note that the stress tensor is symmetric. The constants, α, β, γ are determined by ensuring that the terms in the conservation and constitutive equations balance. The reduced equations are derived from the dimensionless form of equations (1) to (3) excluding terms of 0 (ε^2) and higher.

In order for all the stress terms in the x-momentum equation to survive, the exponent α should be set equal to 2. Correspondingly, setting β = 1 ensures the survival of all the terms in the normal stress equation for q. It can be seen that this results in the streamwise normal stress q not depending strongly on the streamwise elongation term u_x, which should be the case for shear dominated (boundary-layer) flow. However, this stress does not disappear entirely due to the nonlinear coupling with shear effects. With α and β set, the survival of the terms in the shear stress equation for s and normal stress equation for r can be achieved by setting γ = 0. The z-momentum equation now shows that the pressure gradient in the transverse direction is negligible, i.e. $p_z \sim 0(\varepsilon^2)$. This demonstrates that the pressure dependence in the transverse direction is negligible, which is in agreement with the limit of a Newtonian jet flow. Hence, assuming no body forces exist in the transverse direction, the pressure is a function of the streamwise direction and time only. The conservation and constitutive equations are appended to take the following form:

$$u_x+w_z=0 \quad (4)$$

$$Re\left(u_t+uu_x+wu_z\right)=aRvu_{zz}+q_x+s_z+\frac{\varepsilon^3}{Ca}h_{xxx}+G \tag{5}$$

$$De\left(q_t+uq_x+wq_z-2su_z-2qu_x\right)+q=0 \tag{6}$$

$$De\left(r_t+ur_x+wr_z-2sw_x-2rw_z\right)+r=2aw_z \tag{7}$$

$$De\left(s_t+us_x+ws_z-qw_x-ru_z\right)+s=au_z \tag{8}$$

Here, $G=\frac{Re}{Fr^2}$ is the gravity number.

The equations above must be solved subject to the dynamic and kinematic conditions at the free surface, the symmetry conditions at z = 0, and the channel exit conditions at x = 0. The preceding scaling method was applied to the dynamic condition in the normal and tangential directions, resulting in:

$$aRvu_z(x,z=h,t)+s(x,z=h,t)=q(x,z=h,t)h_x(x,t) \tag{9}$$

$$p(x,z=h,t)=-\frac{\varepsilon^3}{Ca}h_{xx} \tag{10}$$

In dimensionless form, the kinematic condition becomes:

$$w(x,z=h,t)=h_t(x,t)+u(x,z=h,t)h_x(x,t) \tag{11}$$

The flow conditions at the channel exit correspond to the flow inside an infinite channel. Thus,

$$\begin{aligned} &u(x=0,z,t)=\frac{1}{2}(3+G)\left(1-z^2\right)\\ &w\left(x=0,z,t\right)=0\\ &q\left(x=0,z,t\right)=2aDez^2\left(3+G\right)^2\\ &r\left(x=0,z,t\right)=0\\ &s\left(x=0,z,t\right)=-az\left(3+G\right)\end{aligned} \tag{12}$$

The jet thickness at the channel exit is assumed fixed, so that

$$h(x=0,z,t)=1 \tag{13}$$

Finally, the symmetry conditions are:

$$w(x,z=0,t)=u_z(x,z=0,t)=s(x,z=0,t)=0 \tag{14}$$

In this formulation it is assumed that no external force or pressure acts on the fluid surface. Also, since the pressure p does not depend on z, the pressure must vanish everywhere. For this reason, the axial pressure gradient term of eq. (5) will no longer be included.

MAPPED EQUATIONS

Traditionally, for Newtonian thin-film flow, the equations are solved by imposing a semi-parabolic profile for the velocity and depth-averaging the equations across the thickness. The strong nonlinear effects originating from inertia and normal stress for a viscoelastic fluid make this approach unfeasible. The solution process is obviously difficult due to the explicit z dependence of the velocity and stress components. Formal handling of the transverse flow expansion was suggested by (Zienkievicz & Heinrich[30] 1979, Ruyer-Quil & Manneville[21] 1998). The present study follows closely and generalizes the work of Zienkievicz & Heinrich[30] (1979), with the exception that the transverse velocity component will not be neglected and the change in surface height over time is also included.

For the solution procedure, the equations are first mapped onto a rectangular domain in order to apply the spectral method. All flow variables are then expanded in terms of polynomial shape functions in the transverse direction. The Galerkin projection is then applied in order to generate the equations that determine the expansion coefficients. A Lagrangian time-stepping implicit finite-difference method is coupled with a fourth-order Runge-Kutta integration solution approach in the flow direction in order to determine the expansion coefficients. This is a similar approach as to the ones developed previously for two-dimensional coating flow of Newtonian (Khayat & Welke[15] 2001), and generalized Newtonian fluids (Khayat and Kim[16] 2002). The present formulation is quite involved and will only be summarized in this paper. Equations (4) to (8) are reduced to a transient one-dimensional problem formulation by an expansion of the velocity and stress components in terms of orthonormal modes in the transverse direction. The following mapping is used:

$$\chi(x,z,t)=x, \quad \xi(x,z,t)=\frac{z}{h(x,t)}, \quad \tau(x,z,t)=t$$

with $\xi \in [0, 1]$.

Let v be a general function variable. Thus, one introduces the convective derivative as

$$\frac{dv}{d\tau}=v_\tau-\frac{\xi}{h}\left(h_\tau v_\xi+uv_\xi h_\chi\right)+uv_\chi+\frac{1}{h}wv_\xi \tag{15}$$

The mapped equations are as follows,

$$u_\chi-\frac{\xi}{h}h_\chi u_\xi+w_\xi\frac{1}{h}=0 \tag{16}$$

$$Re\frac{du}{d\tau}=\frac{1}{h}\left(\frac{aRv}{h}u_{\xi\xi}-\xi h_\chi q_\xi+s_\xi\right)+q_\chi+\frac{\varepsilon^3}{Ca}h_{\chi\chi\chi}+G \tag{17}$$

$$De\left[\frac{dq}{d\tau}-\frac{2}{h}su_\xi-2q\left(u_\chi-\frac{\xi}{h}h_\chi u_\xi\right)\right]+q=0 \tag{18}$$

$$De\left[\frac{dr}{d\tau}+\frac{2}{h}\left(\xi sh_\chi w_\xi-rw_\xi\right)-2sw_\chi\right]+r=\frac{2a}{h}w_\xi \tag{19}$$

$$De\left[\frac{ds}{d\tau}+\frac{1}{h}\left(\xi qh_\chi w_\xi-ru_\xi\right)-qw_\chi\right]+s=\frac{1}{h}au_\xi \tag{20}$$

SPECTRAL EXPANSION

The orthonormal shape functions $A_i(\xi)$, $B_i(\xi)$, $C_i(\xi)$ and $D_i(\xi)$ for the streamwise velocity, u, normal stress component q, and shear component s as well as the normal stress component r are shown as follows:

$$u(\chi,\xi,\tau)=\sum_{i=1}^{M}U_i(\chi,\tau)A_i(\xi),\quad q(\chi,\xi,\tau)=\sum_{i=1}^{M}Q_i(\chi,\tau)B_i(\xi),$$
$$r(\chi,\xi,\tau)=\sum_{i=1}^{M}R_i(\chi,\tau)C_i(\xi),\quad s(\chi,\xi,\tau)=\sum_{i=1}^{M}S_i(\chi,\tau)D_i(\xi),$$

where M represents the number of modes and the unknown coefficients are $U_i(\chi,\tau)$, $Q_i(\chi,\tau)$, $R_i(\chi,\tau)$ and $S_i(\chi,\tau)$. Also, generally, let, $v(\chi,\xi,\tau)=\sum_{i=1}^{M}V_i(\chi,\tau)\psi_i(\xi)$. Equation (16) becomes

$$U_{i\chi}A_i-\frac{1}{h}\left(\xi h_\chi U_i A_i^{'}+w_\xi\right)=0 \tag{21}$$

The transverse velocity component, w, is determined by integrating the continuity equation (2.16) to give:

$$w(\chi,\xi,\tau)=h_\chi\left(\xi A_i\text{-}j_i\right)U_i\text{-}hj_iU_{i\chi} \tag{22}$$

Where, $\phi_i(\xi)=\int_0^{\xi}A_i d\xi$.

In this case, the convective terms are of the following form

$$\begin{aligned}\frac{dv}{d\tau}=&V_{j\tau}\psi_j-\frac{1}{h}V_j\psi_j^{'}\left[\xi\left(h_\tau+h_\chi U_kA_k\right)-h_\chi\left(\xi A_k\text{-}j_k\right)U_k\right]\\&+U_jA_jV_{k\chi}\psi_k-V_j\psi_j^{'}U_{k\chi}j_k\end{aligned} \tag{23}$$

Equations (17) to (20) becomes,

$$\begin{aligned}Re\frac{du}{d\tau}=&\frac{1}{h}\left[\frac{aRv}{h}U_jA_j^{''}-\xi h_\chi Q_jB_j^{'}+S_jD_j^{'}\right]\\&+Q_{k\chi}B_k+\frac{\varepsilon^3}{Ca}h_{\chi\chi\chi}+G\end{aligned} \tag{24}$$

$$\begin{aligned}De\left[\frac{dq}{d\tau}+\frac{2}{h}U_jA_j^{'}\left(\xi h_\chi Q_kB_k\text{-}S_kD_k\right)\text{-}2Q_jB_jU_{k\chi}A_k\right]\\+Q_jB_j=0\end{aligned} \tag{25}$$

$$\begin{aligned}De\Bigg[\frac{dr}{d\tau}+2\sum_{j=1}^{M}S_jD_j\Bigg[h_\chi\left\{\frac{\xi h_\chi}{h}U_k\left(\xi A_k^{'}+A_k\text{-}j_k^{'}\right)\text{-}U_{k\chi}j_k^{'}\right\}\\
\text{-}\left\{\left(\xi A_k\text{-}j_k\right)\left(h_\chi U_k\right)_\chi\text{-}j_k\left(hU_{k\chi}\right)_\chi\right\}\Bigg]\\
\text{-}2R_jC_j\left\{\frac{h_\chi}{h}\left(\xi A_k^{'}+A_k\text{-}j_k^{'}\right)U_k\text{-}U_{k\chi}j_k^{'}\right\}\Bigg]\\
+R_jC_j=\frac{2a}{h}\left[h_\chi\left(\xi A_j^{'}+A_j\text{-}j_j^{'}\right)U_j\text{-}hU_{j\chi}j_j^{'}\right]\end{aligned} \tag{26}$$

$$\begin{aligned}De\Bigg[\frac{ds}{d\tau}+Q_jB_j\Bigg[h_\chi\left\{\frac{\xi h_\chi}{h}U_k\left(\xi A_k^{'}+A_k\text{-}j_k^{'}\right)\text{-}\xi U_{k\chi}j_k^{'}\right\}\\
\text{-}\left\{\left(\xi A_k\text{-}j_k\right)\left(h_\chi U_k\right)_\chi\text{-}j_k\left(hU_{k\chi}\right)_\chi\right\}\Bigg]\\
\text{-}\frac{1}{h}U_jA_j^{'}R_kC_k\Bigg]+S_jD_j=\frac{a}{h}U_jA_j^{'}\end{aligned} \tag{27}$$

where prime denotes a total differentiation.

In addition to the condition of orthonormality, the shape functions must also satisfy various boundary conditions. Some of these conditions are not obvious. One condition is the limit of Newtonian film flow being recovered for this viscoelastic formulation as Rv $\to\infty$. One major difficulty for viscoelastic flow, as opposed to a Newtonian flow, is that the shear stress does not simply and necessarily vanish at the free surface. This becomes apparent when examining condition (9), and also noting that there does not exist separate boundary conditions on shear and normal stresses. This, however, can be remedied by satisfying condition (9) as well as recovering the Newtonian limit by simply setting the shear and normal stresses equal to zero at the free surface. Hence, assuming orthonormality, the following conditions apply for A_i:

$$\left\langle A_iA_j\right\rangle=\delta_{ij},\qquad A_i^{'}(\xi=0)=A_i^{'}(\xi=1)=0 \tag{28}$$

which satisfy conditions (14). Here, δ_{ij} is the Kronecker delta, and $\langle\ \rangle$ denotes the integration over the interval $\xi\in$ [0, 1].

For B_i, It is not difficult to deduce from eq. (6) that, given the symmetry conditions (14), q is also symmetric with respect to the centerline. Thus,

$$\left\langle B_iB_j\right\rangle=\delta_{ij},\qquad B_i'(\xi=0)=0 \tag{29}$$

Note that $q(x,\ z=0)$ does not necessarily vanish, unless $q(x=0,\ z=0)=0$. The boundary conditions for C_i are not as obvious. Nothing for certain can be said about r at either the free surface or line of symmetry. In this case, the corresponding shape function is assumed to satisfy only the condition of orthonormality, namely

$$\left\langle C_i C_j \right\rangle = \delta_{ij} \tag{30}$$

The kinematic condition (11) becomes,

$$h_\chi = -\frac{h}{\overline{U}} U_{i\chi} \left\langle A_i \right\rangle - \frac{h_\tau}{\overline{U}} \tag{31}$$

where, $\overline{U} = U_i \left\langle A_i \right\rangle$.

While carrying out Galerkin Projection, the convective terms become, from eq. (23),

$$\begin{aligned}\left\langle \frac{dv}{d\tau} \psi_i \right\rangle &= V_{i\tau} - \frac{1}{h} V_j \left[h_\tau \left\langle \xi \psi_j' \psi_i \right\rangle + h_\chi U_k \left\langle j_k \psi_j' \psi_i \right\rangle \right] \\ &+ U_j V_{k\chi} \left\langle A_j \psi_k \psi_i \right\rangle - V_j U_{k\chi} \left\langle j_k \psi_j' \psi_i \right\rangle\end{aligned} \tag{32}$$

Equations (24) to (27) become,

$$\begin{aligned}Re \left\langle \frac{du}{d\tau} A_i \right\rangle &= \frac{1}{h} \left(\frac{aRv}{h} U_j \left\langle A_j'' A_i \right\rangle + S_j \left\langle D_j' A_i \right\rangle - h_\chi Q_j \left\langle \xi B_j' A_i \right\rangle \right) \\ &+ Q_{j\chi} \left\langle A_i B_j \right\rangle + \frac{\varepsilon^3}{Ca} h_{\chi\chi\chi} \left\langle A_i \right\rangle + G \left\langle A_i \right\rangle\end{aligned} \tag{33}$$

$$\begin{aligned}De &\left[\left\langle \frac{dq}{d\tau} B_i \right\rangle + \frac{2}{h} U_j \left(h_\chi Q_k \left\langle \xi A_j' B_k B_i \right\rangle - S_k \left\langle A_j' D_k B_i \right\rangle \right) \right. \\ &\left. -2 Q_j U_{k\chi} \left\langle B_j A_k B_i \right\rangle \right] + Q_i = 0\end{aligned} \tag{34}$$

$$\begin{aligned}De &\left[\left\langle \frac{dr}{d\tau} C_i \right\rangle + 2S_j \left[h_\chi \left\{ \frac{h_\chi}{h} U_k \left\langle \xi \left(\xi A_k' + A_k - j_k' \right) D_j C_i \right\rangle \right. \right. \right. \\ &\left. - U_{k\chi} \left\langle \xi j_k' D_j C_i \right\rangle \right\} - \left\{ \left(h_\chi U_k \right)_\chi \left\langle \left(\xi A_k - j_k \right) D_j C_i \right\rangle \right. \\ &\left. \left. - \left(h U_{k\chi} \right)_\chi \left\langle j_k D_j C_i \right\rangle \right\} \right] - 2R_j \left\{ \frac{h_\chi}{h} \left\langle \left(\xi A_k' + A_k - j_k' \right) C_j C_i \right\rangle U_k \right. \\ &\left. \left. - U_{k\chi} \left\langle j_k' C_j C_i \right\rangle \right\} \right] + R_i = \frac{2a}{h} \left[h_\chi \left\langle \left(\xi A_j' + A_j - j_j' \right) C_i \right\rangle U_j \right. \\ &\left. - h U_{j\chi} \left\langle j_j' C_i \right\rangle \right]\end{aligned} \tag{35}$$

$$\begin{aligned}De &\left[\left\langle \frac{ds}{d\tau} D_i \right\rangle + Q_j \left[h_\chi \left\{ \frac{h_\chi}{h} U_k \left\langle \xi \left(\xi A_k' + A_k - j_k' \right) B_j D_i \right\rangle \right. \right. \right. \\ &\left. - U_{k\chi} \left\langle \xi j_k' B_j D_i \right\rangle \right\} - \left\{ \left(h_\chi U_k \right)_\chi \left\langle \left(\xi A_k - j_k \right) B_j D_i \right\rangle \right. \\ &\left. \left. \left. - \left(h U_{k\chi} \right)_\chi \left\langle j_k B_j D_i \right\rangle \right\} \right] - \frac{1}{h} U_j R_k \left\langle A_j' C_k D_i \right\rangle \right] \\ &+ S_i = \frac{a}{h} U_j \left\langle A_j' D_i \right\rangle\end{aligned} \tag{36}$$

Using expression (22), condition (11) becomes,

$$h_\tau + h U_{j\chi} \left\langle A_j \right\rangle + h_\chi U_j \left\langle A_j \right\rangle = 0 \tag{37}$$

The boundary conditions (12) become,

$$\begin{aligned}&U_i(\chi=0,\tau) = \frac{(3+G)}{2} \left\langle \left(1-\xi^2 \right) A_i(\xi) \right\rangle \\ &Q_i(\chi=0,\tau) = 2aDe \left(3+G \right)^2 \left\langle \xi^2 B_i(\xi) \right\rangle \\ &R_i(\chi=0,\tau) = 0, \\ &S_i(\chi=0,\tau) = -a \left(3+G \right) \left\langle \xi D_i(\xi) \right\rangle \\ &h\left(\chi=0,\tau \right) = 1\end{aligned} \tag{38}$$

As long as the boundary and orthonormality conditions are satisfied, it has been found that any number of arbitrary modes can be introduced. This is analogous to Newtonian and generalized Newtonian flows (Khayat & Welke[15] 2001; Kim & Khayat[18] 2002). However, reasonable accuracy is achieved using M > 3.

RESULTS AND DISCUSSION

The formulation and numerical implementation above are now used to study the flow of a thin viscoelastic jet emerging from the channel as illustrated schematically in fig. 1. Although the physical domain of the fluid is assumed to extend from $x = 0$ to $x \to \infty$, but the computational domain will be restricted to $x \in [0, 1]$. The flow of a Newtonian fluid is also examined for reference.

Steady Newtonian Jet Flow

The influence of inertia on steady jet flow is first examined for a Newtonian fluid by varying the Reynolds number from $Re \in [10, 50]$ while assuming negligible gravity ($Fr \to \infty$). The flow is illustrated in fig. 2 with the height of the free surface $h(x)$ and the transverse velocity at the free surface $w(x, z = h)$ plotted against x for a given Reynolds number. Since mass is conserved, the (average) steady streamwise velocity is simply the inverse of the film height, and is therefore not shown. The film profiles in fig. 2a show a monotonic response of the jet thickness, with a strong contraction in film height close to the channel exit. This contraction is strengthened by inertia. The curves in the figure suggest, as expected, that in the limit of infinite Reynolds number, the jet thickness remains constant with x, with plug-flow conditions reached almost immediately downstream from the channel exit. The contraction in height is accompanied by a sharp drop in transverse velocity (fig. 2b), which reaches a minimum at a location close to the channel exit that is essentially independent of inertia. Plug flow conditions are reached far downstream from the channel exit at any Reynolds number.

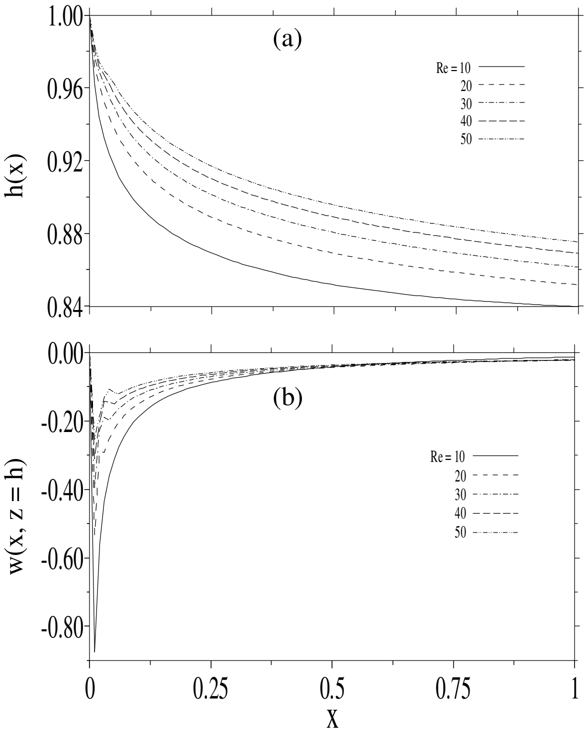

FIGURE 2: INFLUENCE OF INERTIA ON STEADY-STATE NEWTONIAN JET THICKNESS (a), AND SURFACE TRANSVERSE VELOCITY (b) IN THE ABSENCE OF GRAVITY.

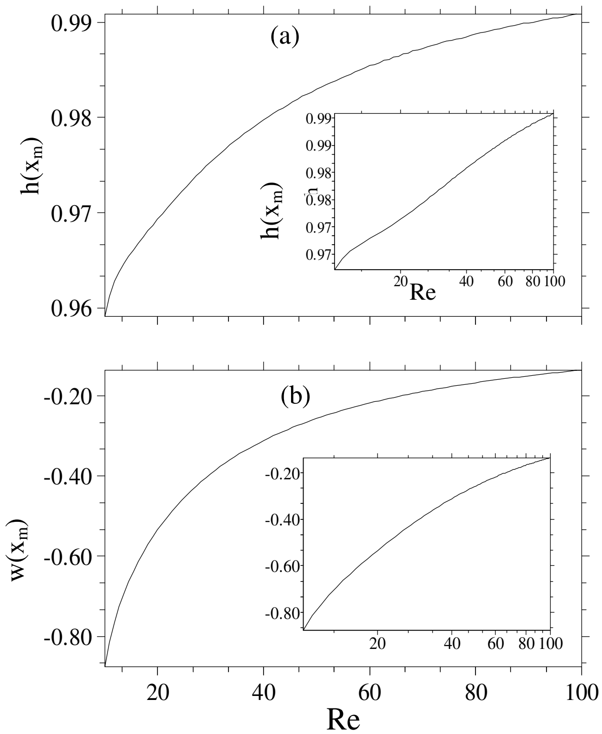

FIGURE 3: JET THICKNESS (a) AND MINIMUM TRANSVERSE VELOCITY (b) FOR A NEWTONIAN JET AS FUNCTION OF INERTIA. (INSET SHOWS SEMI-LOG SCALE) AT THE LOCATION, x_m, OF MINIMUM w.

Further insight on the role of inertia is inferred from fig. 3. The jet thickness and transverse velocity are plotted against Re in fig. 3a and 3b, respectively, at the location, x_m of minimum w or maximum downward flow. The flow response is obviously monotonic with respect to *Re*. The inset in figure 3a indicates that $h(x_m)$ grows like $3.2\times10^{-4}\ln(Re)$. Figures 3a and 3b show that the flow is strongly dependent on inertia for small Reynolds number. In fact, as $Re \to 0$, the jet tends to infinitely contract near $x = 0$, collapsing onto an infinitely thin filament. This behavior is exactly opposite to that encountered in the flow exiting a channel and flowing over a rigid plate (as in coating flow).

As expected, the flow is predominantly in the streamwise direction with plug-flow conditions prevailing for approximately $x > 0.75$. The strength of transverse flow is essentially confined to the free surface near the channel exit. The strong elongational flow, which is particularly evident near $x = 0$, is accompanied by a strong variation of the transverse flow with z.

Steady Viscoelastic Jet Flow

The effect of elasticity can be examined by varying either the viscosity ratio or the Deborah number. In the current work, only De is varied and Rv is set equal to 1 unless otherwise specified.

Figure 4 displays the jet profiles (fig. 4a) and the profiles corresponding to the steady transverse normal stress component at low Reynolds number ($Re = 5.0$) in the absence of gravity. The range of Deborah numbers considered is $De \in [1, 3.4]$. Although the *De* range is narrow, the flow is strongly influenced by elasticity. Figure 4a shows that the level of film contraction near the channel exit is essentially independent of elasticity, but elasticity tends to generally enhance contraction. In contrast to a Newtonian jet, which shows a monotonic decrease in thickness, the viscoelastic jet tends to thicken at a location downstream of the channel exit. The jet thickness exhibits a minimum close to the channel exit and a maximum further downstream. Figure 4a shows that the jet thickness tends to asymptotically converge to a constant level far downstream from the channel exit. In this case, plug flow conditions are reached regardless of the value of *De*. This response is similar to that predicted for a Newtonian jet. Figure 4b shows a significant buildup in normal stress at the jet surface, with r reaching a maximum near $x = 0$. This buildup starts at the channel and is also experienced well below the free surface.

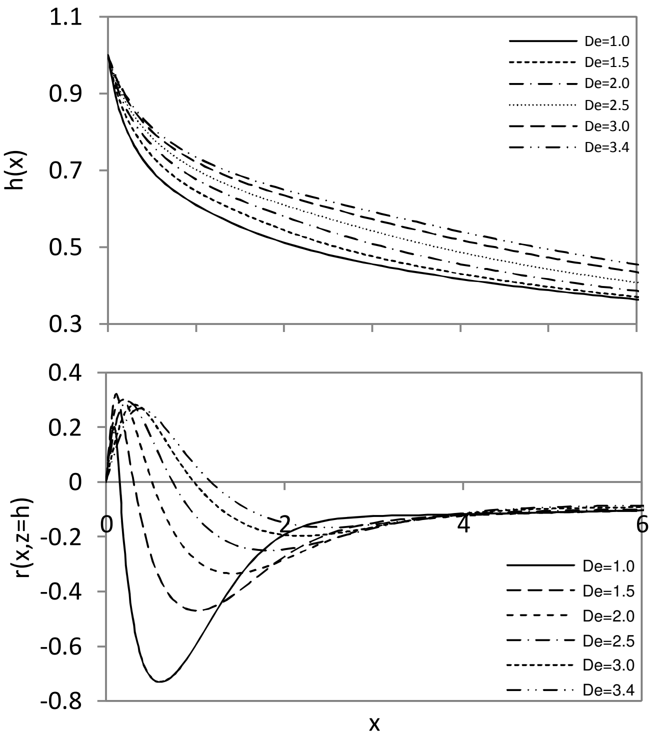

FIGURE 4: INFLUENCE OF ELASTICITY ON STEADY STATE JET THICKNESS (a) AND TRANSVERSE NORMAL STRESS (b) AT THE SURFACE.

Figure 5 displays the profiles for the steady polymeric shear stress averaged over the film thickness. The shear stress exhibits a minimum and a maximum similarly to transverse velocity, whereas the normal stress difference tends to experience a strong minimum. A similar trend is observed from fig. 4b.

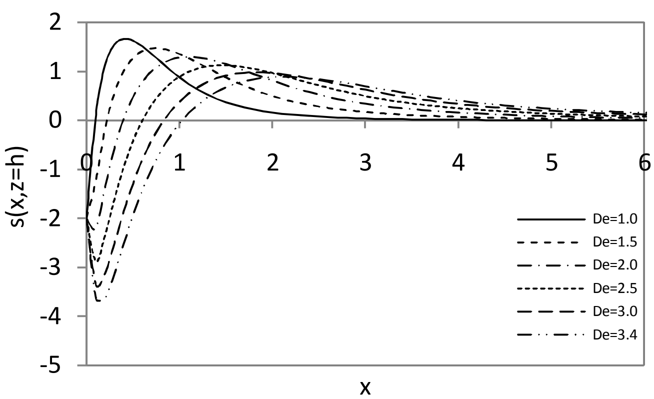

FIGURE 5: INFLUENCE OF ELASTICITY ON AVERAGE SHEAR STRESS.

The onset of waviness in flow and jet thickness is obviously the result of elastic effect. This can be shown by taking a perturbation expansion of the stress components and assuming *De* small. If one examines the stress equations in the vicinity of the free surface, one finds, upon neglecting terms of $0(De^2)$, that eq. (6) and eq. (7) lead to $q \simeq 2aDeu_z^2$ and $s \simeq au_z$, respectively. This indicates that q tends to zero faster than s as the free surface is approached. Simultaneously, eq. (8) indicates that, to leading order, $r \simeq 2aw_z$. In this case, w_X can be estimated from the higher-order (upper-convective) terms.

A major contrast between the Newtonian and viscoelastic jet flows is reflected in the flow field. For a Newtonian jet, the flow becomes fully developed and reaches plug flow conditions only far downstream from the channel exit. In contrast, a viscoelastic jet displays uniform flow much closer to the channel exit, over a relatively deep region below the free surface. Thus, while the boundary-layer region extends over the entire jet thickness for a Newtonian jet, it remains confined to the core region of the viscoelastic jet.

The interplay between the effects of elasticity and inertia is now examined. For a very small increase in *Re* has the effect of lowering the free surface maximum to a relatively large degree. In contrast, the minimum level in the free surface does not appear to vary considerably with *Re*. Overall, the jet profiles, velocity and normal stress distributions suggest that inertia tends to play an opposite role to elasticity. A reduction in inertia level or rise in elasticity level for a viscoelastic jet leads to the emergence of surface waviness and excessive normal stress level. This rise in normal stress leads in turn to the formation of sharp gradients in velocity and shear stress. Thus, at a critical elasticity or inertia level, these gradients can be sufficiently substantial to cause a discontinuity or shock in the flow. Of course, velocity gradients and polymeric stresses are coupled. However, the variation in w and the jump in s appear to be primarily responsible for shock formation. For given *Re*, if *De* is small, the jet surface decreases monotonically with position. As *De* increases, the jet surface exhibits waviness. Beyond a critical *De* value a discontinuity in flow occurs (shock formation). This indicates, expectedly, that a more dilute fluid solution must have a more elastic polymeric solute for the jet to become wavy. Interestingly, the range of waviness is very narrow, and does not seem to depend strongly on *Rv*.

CONCLUSION

The symmetric two-dimensional flow of a thin viscoelastic fluid jet emerging from a vertical channel is examined in this study. The fluid is modeled following the Oldroyd-B constitutive model, with the influence of inertia and elasticity investigated for steady flow. The thin-film equations are solved by expanding the flow field and stresses in terms of orthonormal modes in the transverse direction using the Galerkin projection. In contrast to the depth-averaging technique, the proposed method predicts the shape of the free surface, as well as the velocity and stress components within the fluid.

For a steady Newtonian jet the jet thickness remains essentially constant with x for large Reynolds number. However, the flow is strongly dependent on inertia for small Reynolds number with the jet tending to contract and collapse onto a thin line as Re approaches 0. The thickness for a Newtonian jet was shown to vary only monotonically, whereas a viscoelastic jet tends to thicken downstream of the channel exit. Steady Newtonian jet flow becomes fully developed only far downstream from the channel exit. In contrast, a viscoelastic jet displays uniform flow much closer to the channel exit and over a relatively deep region below the free surface. For a steady viscoelastic jet, a reduction in inertia or a rise in elasticity leads to the emergence of surface waviness and excessive normal stress. This rise in normal stress leads to the formation of sharp gradients in the velocity and shear stress. These gradients can be sufficiently substantial to cause a discontinuity or shock in the flow. The wavy region that precedes the onset of shock or jet rupture is very thin, which illustrates how rapidly the jet surface evolves from a monotonic to a ruptured film.

ACKNOWLEDGMENTS

This work is supported by the Natural Sciences and Engineering Research Council (NSERC) of Canada.

REFERENCES

[1] Alekseenko, S. V., Nakoryakov, V. E., Pokusaev, B. G. 1985 Wave Formation On A Vertical Falling Liquid Film. AIChE J. **31**: 1446.

[2] Benney, D. J. 1966 Long Waves in Liquid Films. J.Math, Phys. **45**: 150.

[3] Bérdaudo, C., Fortin, A., Coupez, T., Demay, Y., Vergnes, B., Agassant, J.F. 1998 A Finite Element Method For Computing The Flow Of Multi-Mode Viscoelastic Fluids: Comparison With Experiments. J. Non-Newtonian Fluid Mech. **75**: 1.

[4] Bertschy, J. R., Chin, R.W. & Abernathy, F.H. 1993 High-Strain-Rate Free-Surface Boundary- Layer Flows. J. Fluid Mech. **216**: 443.

[5] Bird, R. B., Armstrong, R. C. & Hassanger, O. 1987 Dynamics Of Polymeric Liquids, Vol. 1, 2nd edn., JohnWiley.

[6] Bousfield, D. W., Keunings, R., Marrucci, G. & Denn, M. M. 1986 Nonlinear Analysis Of The Surface Tension Driven Breakup Of Viscoelastic Filaments. J. Non-Newtonian Fluid Mech. **21**: 79.

[7] Chang, H.-C., Demekhin, E. A., Kopelevich, D.I. 1993 Nonlinear Evolution Of Waves On A Falling Film. J. Fluid Mech. **250**: 433.

[8] Chang, H.-C. 1994 Wave Evolution on A Falling Film. Annu. Rev. Fluid Mech. **26**: 103.

[9] Christanti, Y. & Walker, L. M. 2001 Surface Driven Jet Break Up Of Strain Hardening Polymer Solutions. J. Non-Newtonian Fluid Mech. **100**: 9.

[10] Demekhin, E. A., Shkadov, V. Ya. 1985 Two-Dimensional Wave Regimes Of A Thin Liquid Film. Izv. Akad. Nauk Sssr, Mekh. Zhidk. Gaza **3**: 63.

[11] German, R., Khayat, R. E. 2005 Steady And Transient Thin-Jet Flow. Phys. Fluids **17**:102104.

[12] Frenkel, A. L. 1992 Nonlinear Theory Of Strongly Undulating Thin Films Flowing Down Vertical Surfaces. Europhys, Letts. **18**:583.

[13] Kang, F., Chen, K.P. 1995 Nonlinear Elastic Instability Of Gravity-Driven Flow Of A Thin Viscoelastic Film Down An Inclined Plane. J. Non-Newtonian Fluid Mech. **57**: 243.

[14] Khayat, R. E. 2001 Transient Two-Dimensional Coating Flow Of A Viscoelastic Fluid Film On A Substrate Of Arbitrary Shape. J. Non-Newtonian Fluid Mech. **95**: 199.

[15] Khayat, R. E., Welke, S. 2001 Influence Of Inertia, Gravity And Substrate Topography On The Two-Dimensional Transient Coating Flow Of A Thin Newtonian Fluid Film. Phys. Fluids **13**: 355.

[16] Khayat, R. E., Kim, K. 2002 Influence Of Initial Conditions On Transient Two-Dimensional Thin-Film Flow. Phys. Fluids. **14**:4448.

[17] Khayat, R. E., Kim, K. 2006 Thin-Film Flow Of A Viscoelastic Fluid On An Axisymmetric Substrate Of Arbitrary Shape. J. Fluid Mech. **552**:31.

[18] Kim, K. & Khayat, R. E. 2002 Influence Of Non-Newtonian Effects On The Transient Flow Of A Thin Fluid Film. Phys. Fluids. **14**:2202.

[19] Kriegsmann, J. J., Mikis, M. J. & Vanden-Broek, J. 1998 Pressure Driven Disturbances On A Thin Viscous Film. Phys. Fluids **10**: 1249.

[20] Liang, Y., Oztekin, A., Neti, S. 1995 Dynamics of Viscoelastic Jets Of Polymeric Liquid Extrudate. J. Non-Newt. Fluid Mech. **81:** 105.

[21] Ruyer-Quil, C. & Manneville, P. 1998 Modeling Film Flows Down Inclined Planes. *Eur. J. Phys.* **6**: 277.

[22] Shkadov, V. Y. 1967 Wave Conditions Of A Flow In A Thin Viscous Layer Under The Action Of Gravitational Forces. Izv. Akad. Nauk. Sssr Mehk, Zhid. Gaza **1:** 43.

[23] Tauqeer Muhammad & Khayat, Roger E. 2004 Effect Of Substrate Movement On Shock Formation In Pressure-Driven Coating Flow. Phys. Fluids **16**: 1818.

[24] Tome, M. F., Duffy, B. & Mckee, S. 1996 A Numerical Technique For Solving Non-Newtonian Free Surface Flow. J. Non-Newtonian Fluid Mech. **62**: 9.

[25] Trang-Cong, T. & Phan-Thien, N. 1988 Three-Dimensional Study Of Extrusion Processes By Boundary-Element Method. Ii. Extrusion Of A Viscoelastic Fluid. Rheol. Acta **27**: 639.

[26] Trivfonov, Yu., Tsvelodu, O., Yu. 1991 Nonlinear Waves On The Surface of A Falling Liquid Film Part I. J. Fluid Mech. **229**: 531.

[27] Watson, E. J., 1964 The Radial Spread Of A Liquid Jet Over A Horizontal Plane. J. Fluid Mech. **20**: 217.

[28] Wilkes, J. O., Nedderman, R. M. 1962 The Measurement Of Velocities In Thin Film Of Liquid. Chem. Eng. Sci. **17**: 177.

[29] Zhang, Y. L., Matar, O. K. & Craster, R. V. 2002 Surfactant Spreading On A Thin Weakly Viscoelastic Film. J. Non-Newtonian Fluid Mech. **105**: 53.

[30] Zienkievicz, O. C. & Heinrich, J. C. 1979 A Unified Treatment of Steady-State Shallow Water And Two-Dimensional Navier–Stokes Equations–Finite-Element Penalty Function Approach. Comput. Meth. Appl. Mech. Eng **17/18**: 673.